Synthetic and Systems Biotechnology 9 (2024) 242–249

Contents lists available at ScienceDirect

Synthetic and Systems Biotechnology

journal homepage: www.keaipublishing.com/en/journals/synthetic-and-systems-biotechnology

Biosensor-assisted CRISPRi high-throughput screening to identify genetic targets in *Zymomonas mobilis* for high D-lactate production

Qiqun Peng [1], Weiwei Bao [1], Binan Geng [**], Shihui Yang [*]

State Key Laboratory of Biocatalysis and Enzyme Engineering, and School of Life Sciences, Hubei University, Wuhan, 430062, China

ARTICLE INFO

Keywords:
D-lactate
Biosensor
LldR
Genome-wide CRISPRi
FACS
Zymomonas mobilis

ABSTRACT

Lactate is an important monomer for the synthesis of poly-lactate (PLA), which is a substitute for the petrochemical plastics. To achieve the goal of high lactate titer, rate, and yield for commercial production, efficient lactate production pathway is needed as well as genetic targets that affect high lactate production and tolerance. In this study, an LldR-based D-lactate biosensor with a broad dynamic range was first applied into *Zymomonas mobilis* to select mutant strains with strong GFP fluorescence, which could be the mutant strains with increased D-lactate production. Then, LldR-based D-lactate biosensor was combined with a genome-wide CRISPR interference (CRISPRi) library targeting the entire genome to generate thousands of mutants with gRNA targeting different genetic targets across the whole genome. Specifically, two mutant libraries were selected containing 10^5 and 10^4 mutants with different interference sites from two rounds of fluorescence-activated cell sorting (FACS), respectively. Two genetic targets of *ZMO1323* and *ZMO1530* were characterized and confirmed to be associated with the increased D-lactate production, further knockout of *ZMO1323* and *ZMO1530* resulted in a 15% and 21% increase of D-lactate production, respectively. This work thus not only established a high-throughput approach that combines genome-scale CRISPRi and biosensor-assisted screening to identify genetic targets associated with D-lactate production in *Z. mobilis*, but also provided a feasible high-throughput screening approach for rapid identification of genetic targets associated with strain performance for other industrial microorganisms.

1. Introduction

Poly-lactate (PLA) is a biodegradable polymer with great potential to be a substitute of the petroleum-based plastics and help reduce environmental pollution [1]. As a building block for the production of PLA, lactate has gained increasing attentions. The global lactate market was estimated at USD 3.36 billion in 2023 and is projected to expand at a compound annual growth rate of 8.1% from 2024 to 2030 [2]. About 90% of lactate is produced by microbial fermentation, but current lactate production is unable to meet the fast-growing market demand [3]. The abundant renewable raw feedstocks such as lignocellulosic biomass from agricultural residues [4] are promising substrates for economic lactate production at large scales [5]. However, these lignocellulosic materials are difficult for microbial fermentation because different inhibitors were produced during pretreatment, enzymatic hydrolysis, and fermentation processes [6], such as furan derivatives, weak acids, and phenolic compounds [7]. These inhibitors could reduce microbial cell viability and increase production costs [8]. Therefore, it is crucial to explore and develop robust microbial cell factories for economic lignocellulosic lactate production.

Zymomonas mobilis has been developed as an ideal industrial microbial chassis for lignocellulosic bioproducts [9,10] due to its attractive characteristics including inhibitor tolerance [11], acid resistance [12], high-temperature resistance [13], and rapid sugar catabolism with unique anaerobic Entner-Doudoroff (ED) pathway [9], which is beneficial for the production of industrial bioproducts using biomass resources. Multiple bioproducts including cellulosic ethanol, 2, 3-butanediol, and D-lactate have been produced by *Z. mobilis* utilizing lignocellulosic hydrolysates as the carbon sources [14,15]. Furthermore, genome editing toolkits including both heterologous and native

Peer review under responsibility of KeAi Communications Co., Ltd.
* Corresponding author.
** Corresponding author.
E-mail addresses: QiqunPeng@stu.hubu.edu.cn (Q. Peng), WeiweiBao@stu.hubu.edu.cn (W. Bao), binangeng@stu.hubu.edu.cn (B. Geng), Shihui.Yang@hubu.edu.cn (S. Yang).
[1] These authors contributed equally.

https://doi.org/10.1016/j.synbio.2024.02.002
Received 28 December 2023; Received in revised form 4 February 2024; Accepted 4 February 2024
Available online 13 February 2024

CRISPR-Cas systems were continuously developed [16,17], and the establishment of CRISPRi system in diverse microorganisms also gives more genetic manipulation possibilities for synthetic microbial chassis development [18–23].

The heterologous D-lactate metabolic pathway has been constructed in *Z. mobilis* ZM4 through metabolic engineering, and the recombinant strain can produce 42.8 g/L D-lactate using the corncob residue hydrolysate [15]. However, the capability of this recombinant strain to produce D-lactate is rather limited, and the performance of this strain has to be improved for industrial production. Similar to other lactate-producing strains, the improvement of recombinant strains often involves the optimization of the gene expression levels of metabolic pathways and transport proteins [24,25]. Specifically, screening target genes and intentionally enhancing or deleting them to improve the D-lactate titer or tolerance of strains [26–29]. However, the limitations of this approach on design rationality, method universality, and data volume lead to the potential failure of the results to meet expectations because the scope of gene manipulation is often local rather than global while the metabolic network is often receiving complicated regulations [30]. Local modifications often fail to affect the overall metabolic and regulatory networks, and a high-throughput global network manipulation method is essential for efficient strain optimization. The construction of a CRISPRi library at a genome-scale allows for the global regulation of the metabolic network, which can convert metabolite concentrations into fluorescent outputs by combining with metabolite biosensors, and therefore facilitating high-throughput screening of candidate strains with over-production phenotypes to provide a comprehensive solution for regulating the metabolic network.

Biosensor-assisted CRISPRi high-throughput screening that combines a CRISPR interference and a biosensor-mediated screening is a global screening method that has been used to obtain recombinant strains for biochemical production such as coumaric acid and butyrate with high titer, rate, or yield [31]. Specifically, metabolite biosensors can convert metabolite compound concentrations into fluorescence output or cell growth advantages at a single-cell level, and then achieve high-throughput screening of specific high-yield strains through FACS [32–34]. CRISPRi library mediated stringent gene repression could obtain a variety of strains with different gene expressions. A high-throughput method screening for over-production phenotypes has been established in *E. coli* [31], and multiple target genes were identified with the assistance of metabolite biosensors through high-throughput screening and sequencing.

Biosensors for lactate have been mined and characterized. The design principles of these biosensors can be roughly divided into lactate utilization (lld) operon-mediated biosensors and lactate binding proteins (BP) mediated biosensors. The former one based on a lactate catabolic operon (lldP-dld-II) that is negatively regulated through the inversely transcribed *lldR* (encoding a GntR-type regulator), where the repression is released by the supplementation of lactate. Operons to utilize lactate have been characterized from *Escherichia coli*, *Cupriavidus necator* and *Pseudomonas* species [35], and can be used to design a biosensor to sense lactate and then to activate gene expression in response to lactate induction. The latter one based on the combination of BP with the fluorescent protein (FP), binding to lactate causes a conformational change in the BP, thereby altering the chromophore environment and fluorescence intensity of the FP. A BP-based biosensor eLACCO1.1 was characterized with high performance in the extracellular milieu but have a strict requirement for Ca^{2+}, and did not function in the cytosolic environment [36] In summary, lldR-based biosensors are more desirable as they exhibit enhanced responsiveness to intracellular lactate production.

In this study, an LldR-based D-lactate biosensor was used to develop the biosensor-assisted CRISPRi high-throughput screening system, which was then applied to identify genetic targets with significant improvements on D-lactate production.

2. Materials and methods

2.1. Strains, media, and chemicals

All strains, plasmids, and primers used in this study are listed in Tables S1–S3. *E. coli Trelief 5α* (Tsingke, Beijing, China) was used for plasmid construction and storage. *Z. mobilis* ZM4 and its derivatives were cultivated in rich media supplemented with 5% glucose (RMG5, 50 g/L glucose, 10 g/L yeast extract, 2 g/L KH_2PO_4) at 30 °C. *E. coli Trelief 5α* was cultured in Luria-Bertani (LB) medium (10 g/L NaCl, 10 g/L tryptone, 5 g/L yeast extract) at 37 °C, 250 rpm. The antibiotics of spectinomycin (100 μg/mL) and chloramphenicol (100 μg/mL) were used for *E. coli* or *Z. mobilis* when required, respectively.

2.2. Plasmid and strain construction

Gibson assembly method [38] was utilized for all plasmid construction. All constructs used in the study are listed in Tables S1–S2. Primers were designed to contain 15-20 nucleotides (nts) overlapping regions with adjacent DNA fragments. The oligonucleotides of primers were ordered from TsingKe Biotechnology Co., Ltd. (Beijing, China). Sequences of the primers are listed in Table S3. Plasmid DNA was extracted using *Trelief* plasmid mini kits plus (TsingKe, Beijing, China). DNA polymerase was purchased from PrimeSTAR (Takara, Kyoto, Japan). Recombinants were confirmed by PCR and Sanger sequencing (Sango, Shanghai, China).

2.3. Electroporation transformation and strain selection

The preparation of electrocompetent cells and electroporation for *Z. mobilis* was carried out following published procedures [39]. Briefly, a single colony was inoculated into 5 mL RMG5 and grown without shaking at 30 °C for 24 h as the seed culture. The seed culture was then transferred to a 250 mL conical flask containing 100 mL of RMG5. Cells were collected by centrifuging when $OD_{600\ nm}$ reached 0.4–0.6. Cell pellets were washed once with sterile water, re-centrifuged, and washed twice in sterilized 10% (v/v) glycerol. These pellets were resuspended in 10% glycerol at a concentration approximately 1000-fold higher than the starting culture. Competent cells were stored at −80 °C as small aliquots for later use. *Z. mobilis* cells were transformed with plasmids by electroporation (Bio-Rad Gene Pulser, 0.1-cm gap cuvettes, 1.8 kV, 200 Ω, 25 μF). After electroporation, 1 mL RMG5 was added to the electroporation mixture and cells were allowed to be recovered at 30 °C for 4–6 h. The revived culture was plated on RMG5 plates containing appropriate antibiotics and then incubated at 30 °C for 2–3 days. Colonies with correct PCR product sizes were selected as candidates and confirmed using Sanger sequencing (Sangon, Shanghai, China).

2.4. Biosensor dynamic range test

To test the dynamic range or substrate scope of engineered biosensor systems, plasmids harboring the biosensor systems were transferred into ZM4-Cas12a Three independent colonies of each testing group were randomly picked and inoculated into 3 mL fresh RMG5 (with appropriate antibiotics) as seed cultures. After 24 h cultivation in a 30 °C rotatory shaker at a speed of 100 rpm, seed cultures were transferred into 3 mL fresh RMG5 with an initial $OD_{600\ nm}$ value of 0.1, gradient concentrations of D-lactate (0–10 g/L) were supplemented into the cultures. After 12 h cultivation, cultures were sampled and subjected to measurement of cell density ($OD_{600\ nm}$) using a UV spectrophotometer (UV-1800, Aoyi, Shanghai, China).

Cells were washed with PBS twice and further resuspended into PBS, and then analyzed by Beckman CytoFLEX FCM flow cytometer (Beckman Coulter, USA). The GFP fluorescence was excited with the 488 nm and detected with FITC, at least 20,000 events of each sample were analyzed to avoid rare events that could affect the population

distribution [40]. Data were processed via CytExpert 2.0 software (Beckman Coulter, USA). The mean fluorescence intensity of triplicates was calculated.

2.5. FACS high-throughput screening

CRISPRi plasmid library was transformed into *Z. mobilis* ZM4-Cas12a-Dldh (pEZ-lldR-P_{lldp}-GFP) to construct a library for identification of genetic targets associated with D-lactate production, and the transformants were then washed twice and resuspended in 1 × PBS buffer with a final cell density of 10^7 cells. The 10^5 cells with the strongest fluorescence intensity were sorted using MoFlo XDP (Beckman Coulter, USA) high-speed flow cytometry sorter with gates set on 510:20 nm emission filters. A 488 nm laser was used for excitation. Forward-scatter characteristics (FSC) was recorded as small-angle scatter, and side-scatter characteristics (SSC) was recorded as orthogonal scatter of the 488 nm laser [41,42]. Secondarily gated was performed using the 0° detector to sort strains with high fluorescence intensities. The sorted cells were then cultivated in the test tubes and spread on RMG5 plates with the corresponding antibiotics.

2.6. Construction of CRISPRi plasmid library

CRISPRi plasmid library was designed based on the ZM4 genome annotation [43], targeting template strands and non-template strands of 1946 genes and 1363 intergenic regions. The design criteria were as follows: all 5′-TTV sites in the genome were identified as PAM sites, and the 23-base sequences after the PAM site were designated as the crRNA sequence. Each gene coding region could be designed with a maximum of 15 crRNAs, and each intergenic region could be designed with a maximum of 6 crRNAs. A total of 2000 crRNAs were included in the negative control, resulting in a total of 69,093 crRNAs. The construction of the pEZ-sgr plasmid followed the previous protocol, and the construction of plasmid library pEZ-sgr-lib was performed by Genewiz (Suzhou, China).

2.7. Deletion of target genes using native I–F CRISPR-Cas system

Editing plasmid pl2r and derivatives were constructed following previous study [17]. Briefly, oligonucleotides were designed according to the targeting sequence, and the targeting crRNA sequence was annealed using two single−stranded oligonucleotides by first heating the reaction mixture to 95 °C for 5 min and subsequently cooling down gradually to room temperature. Then, the annealed spacer was ligated into pl2r that was digested with *Bsa* I. Gibson assembly method was utilized for donor construction. Donor sequences including extra ~800 bp upstream and downstream flank sequences of the candidate gene were amplified using Primer STAR polymerase (Takara, Kyoto, Japan) with genomic DNA of *Z. mobilis* ZM4, and then cloned into corresponding pl2r plasmid.

2.8. Identification of target gene deletion in Z. mobilis

To confirm the deletion of target genes in *Z. mobilis*, mutant candidates were identified by colony PCR. A pair of primers was designed to amplify the region including upstream of the corresponding gene, targeting gene, and downstream of the corresponding gene. Candidate mutants with correct PCR product sizes were selected and confirmed by Sanger sequencing (Sangon, Shanghai, China).

2.9. Curing of targeting plasmids

In order to cure the editing plasmid, the mutant harboring the targeting plasmid after genome editing was inoculated into RMG5 medium without antibiotics selection pressure for 8–16 h, which was then spread on RMG5 plates without antibiotics. Colonies were confirmed as targeting plasmid cured by determining their sensitivity to the corresponding antibiotics.

2.10. Analytical methods

Cell growth was determined by measuring $OD_{600\ nm}$ using a UV spectrophotometer (UV-1800, Aoyi, Shanghai, China). To analyze the profile of metabolites, 1 mL culture supernatants were collected and filtered through a 0.22 μm syringe filter. The concentrations of glucose, D-lactate, and ethanol were determined by high-performance liquid chromatography (HPLC) using the Shimadzu HPLC system (Kyoto, Japan) equipped with a Bio-Rad Aminex HPX-87H column (300 mm × 7.8 mm, 5 μm, Bio-Rad, CA, USA) at 60 °C and refractive index (RI) detector for compound separation and detection, respectively. H_2SO_4 (5 mM) at a flow rate of 0.5 mL/min was used as the mobile phase, following the previous protocol [39].

3. Results

3.1. Establishment and evaluation of D-lactate biosensor system for lactate quantification

A D-lactate inducible system from *Pseudomonas fluorescens* A506 [37] was selected for constructing a D-lactate biosensor in this study to reflect D-lactate concentration in *Z. mobilis*. This system consists of two main components, D-*lldR* encodes a GntR-type regulator that can bind to the P_{lldp} promoter of D-lactate catabolic operon and repress gene expression. The repression will be released when D-lactate is supplemented and binds to D-*lldR* (Fig. 1A). The D-*lldR* gene is driven by a constitutive promoter, and GFP under the control of the P_{lldp} promoter was assembled into pEZ15A, resulting in pEZ-lldR-P_{lldp}-GFP.

To evaluate the accuracy of the biosensor D-*lldR*-P_{lldp} in D-lactate detection, the correlation between D-lactate concentrations and GFP fluorescence intensities was examined. The plasmid harboring biosensor system was transformed into *Z. mobilis* ZM4-Cas12a for the dynamic range test. The transformants were then cultivated with the supplementation of gradient concentrations of D-lactate (0, 2, 4, 6, 8, and 10 g/L). Meanwhile, experiment was carried out to investigate potential cellular metabolism of lactate. Consistent with previous study [44], our results indicated that no lactate was produced or consumed in ZM4-Cas12a during anaerobic cultivation (Fig. S2). The fluorescence intensities increased gradually with the increase of D-lactate concentrations within the range of 3–9 g/L, and the fluorescence intensity was 23.5 times higher in the presence of 9 g/L D-lactate than that without lactate (Fig. 1B). Meanwhile, D-lactate concentrations and GFP fluorescence intensities had a good correlation with a correlation coefficient of 0.98 (Fig. 1C). Therefore, the biosensor system pEZ-lldR-P_{lldp}-GFP is suitable to select recombinant strains with high titer of D-lactate producer in *Z. mobilis*.

3.2. Design and establishment of D-lactate biosensor-assisted CRISPRi high-throughput screening system to identify genetic targets associated with high D-lactate production

D-Lactate biosensor was further combined with a dCas12a mediated genome-wide CRISPRi library to establish a D-lactate biosensor-assisted CRISPRi high-throughput screening system. The dCas12a CRISPRi library contains 69,093 crRNAs targeting 1946 genes in the *Z. mobilis* genome with an average coverage of 15 crRNAs per gene (Fig. 2A), which was transformed into the recombinant strain ZM4-Cas12a-Dldh (pEZ-lldR- P_{lldp} -GFP) containing the D-lactate biosensor to perform genome-wide interference (Fig. 2B).

Since the fluorescence intensity is linked to D-lactate titer in the D-lactate biosensor system, the potential recombinant strains with high GFP fluorescence intensities were sorted in the first round through FACS. The sorted cells were then undergone the second round of FACS

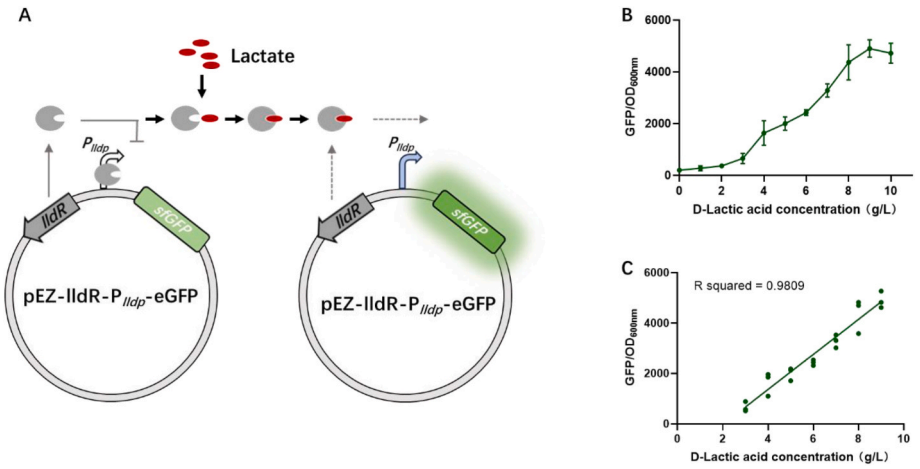

Fig. 1. Design and performance of the D-lactate biosensor system. The D-*lldR* gene is driven by a constitutive promoter, and *sfGFP* is under the control of the promoter P_{lldp}. D-*lldR* binds and occupies the promoter P_{lldp} repressing the expression of *sfGFP* gene. The repression is relieved by the supplementation of D-lactate, which can bind with D-*lldR* releasing it from binding with P_{lldp} (A). Dynamic range test (B) and correlation of GFP induction with different concentrations of D-lactate (C) for the D-*lldR*-P_{lldp} biosensor system. Values are the means of experiments with three technical replicates, error bars are standard deviations.

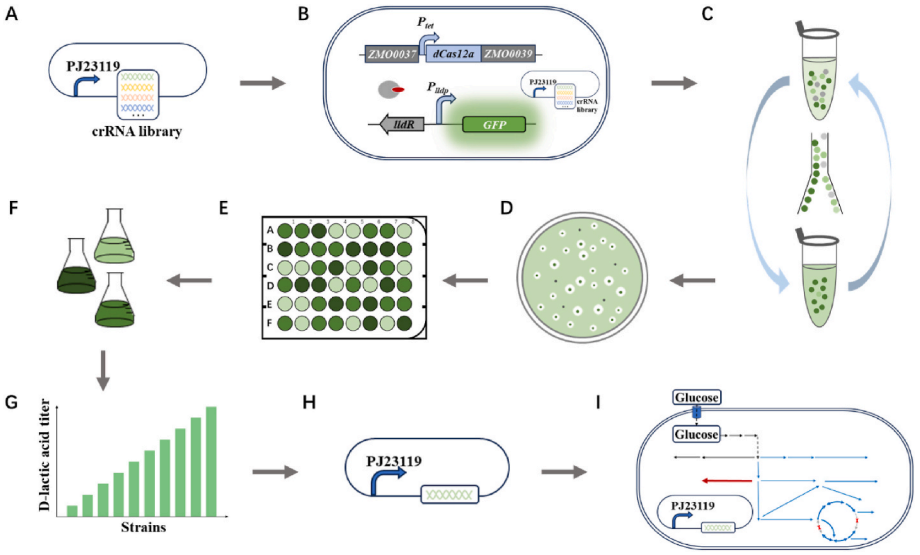

Fig. 2. Schematic diagram of establishment and application of D-*lldR*-P_{lldp} biosensor-assisted CRISPRi high-throughput screening system. The establishment and application of biosensor-assisted genome-wide CRISPRi library involves crRNA library establishment (A), genome-wide interference (B), two rounds of FACS screening (blue arrows represent the second round) (C), plate transparent zone screening(D), strain culturing (E), fermentation test (F), data analysis (G), genetic target identification (H), and rational modification (I).

sorting. All sorted cells from above two rounds FACS sorting were selected as the candidates for high D-lactate production (Fig. 2C), which were then cultivated separately and spread on the plates supplemented with calcium carbonate. Colonies with large transparent zones were selected as the candidate high D-lactate production strains (Fig. 2D). These colonies were further fermented by shake flasks to determine D-lactate production (Fig. 2E and F). The crRNA sequences in strains with increased D-lactate titers were obtained by Sanger sequencing (Fig. 2G), and rational modifications were then carried out based on the identified genes (Fig. 2H).

After the first round of FACS, 10^5 cells with the strongest fluorescence intensities were selected, and 96 colonies with large transparent zones on the plate supplemented with calcium carbonate were further fermented in shake flasks. Approximately 62.5% of the strains had higher D-lactate titers than the control strain with 6.28 g/L (Fig. 3A). The average D-lactate titer of the selected strains is 6.63 g/L with the highest D-lactate titer of 9.31 g/L (Fig. 3B).

To further screen out strains with strong fluorescence intensities, the cells sorted from the first round of FACS were cultured for another round of FACS following the procedures mentioned above. Approximately 10^4 cells with the strongest fluorescence intensities were sorted. And then 96 colonies with obvious transparent zones were picked for the fermentation test. Approximately 97.9% of the strains have higher D-lactate titer than the control with 6.31 g/L (Fig. 3C). The average D-lactate titer of the selected strains in the second round is 7.99 g/L with the highest D-lactate titer of 11.1 g/L (Fig. 3D), the results showed a 20.51% and 19.23% increase in the average and highest D-lactate titer, respectively. With the assistance of biosensor, a strain library with better D-lactate performance was obtained through further selection. Our results indicated that D-lactate concentration was positively converted into fluorescence output, and strains with higher D-lactate titer have been effectively selected by FACS.

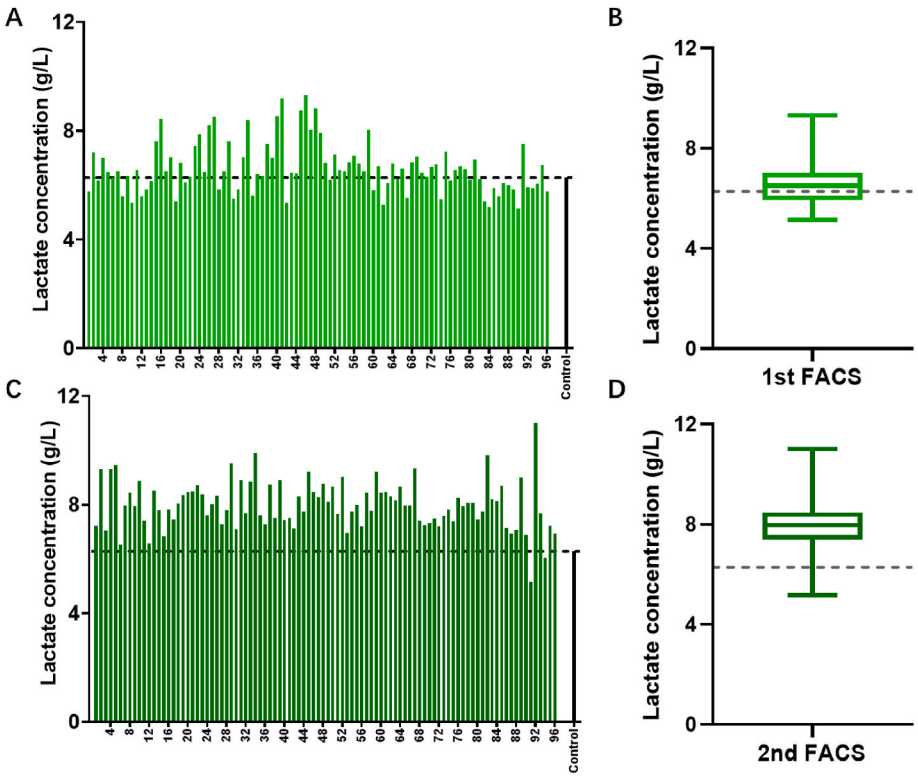

Fig. 3. Titers of D-lactate of mutant D-lactate producers with selected crRNA variants in shake flasks. D-lactate titers (A) and the statistical analysis of D-lactate titers (B) of the mutant strains sorted from the first round of FACS, as well as D-lactate titers (C) and the statistical analysis of D-lactate titers (D) of the mutant strains sorted from the second round of FACS.

3.3. Validation of selected crRNA

To further evaluate that high D-lactate titers of the screened strains were the result of CRISPRi, we cured CRISPRi plasmids and further verified their D-lactate production. 13 strains with a significant increase in D-lactate titers were selected for validation and further analysis. Fermentation experiments were conducted between the superior strains with or without the CRISPRi plasmid to evaluate whether the change in D-lactate titer is caused by CRISPRi. With the presence of interfering plasmid, the D-lactate titer of these strains varies from 8.61 g/L to 11.3 g/L, improved by 38%–54% compared to the control. With the absence of interfering plasmid, the D-lactate titer of these strains was reduced to about 6.31 g/L, which was similar to that of the control (Fig. 4). Our results thus demonstrated that the interference on specific targets

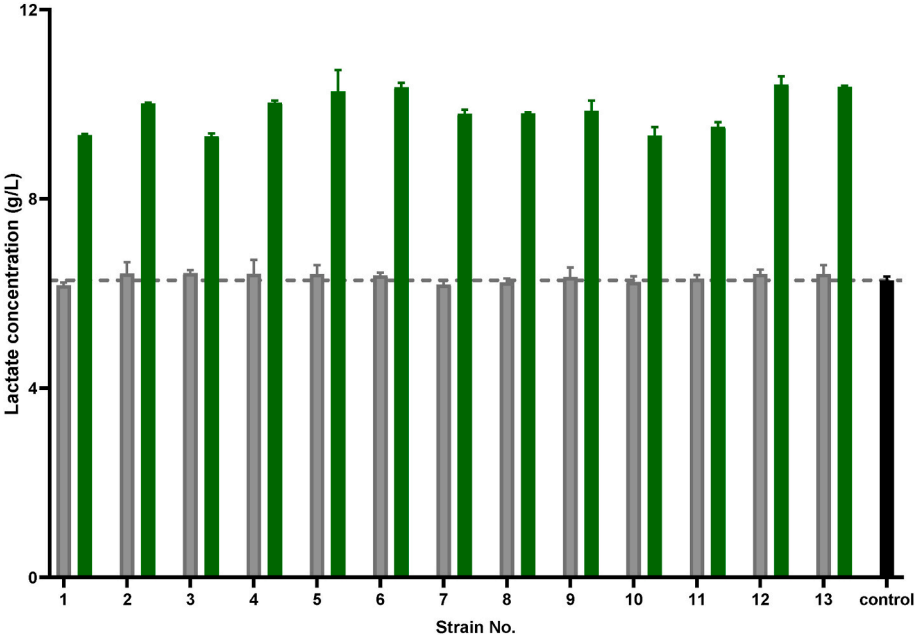

Fig. 4. Comparison of D-lactate titer among the 13 strains containing the CRIPSRi plasmid (shown in green) and the corresponding strains with the CRISPRi plasmid cured (shown in gray). Values are the means of experiments with three technical replicates, error bars are standard deviations.

through CRISPRi led to an improvement in the D-lactate titer.

3.4. Application of target genes

To make a thorough inquiry into the changes in D-lactate titer of these superior strains, PCR amplification and Sanger sequencing were conducted. Thirteen target genes were identified and evaluated with gene-knockout experiments (Table S4). The functions of these genes include transport proteins, signal transduction, and metabolic regulation. CRISPRi on these genes therefore may facilitate the extracellular transport of lactate, enhance resistance to biological stress, and reduce the competing metabolic pathways or other non-essential functions to enhance the D-lactate metabolic pathway, resulting in the increase of D-lactate titer. The relatively high-titer D-lactate producing strain HAPL obtained through metabolic engineering from our early study was applied to further verify and explore the impact of knocking out these genes on D-lactate production.

Nine deletion mutants were then successfully constructed to investigate the effect of these genes on D-lactate titer using type I–F CRISPR-Cas system. The results showed that the D-lactate titer, glucose consumption rate, and biomass of *ZMO1323* deletion strain were all improved, while the *ZMO1044, ZMO0876* and *ZMO0902* deletion strains showed no significant change compared with the control (Table 1, Fig. 5A). Moreover, *ZMO0062, ZMO0023,* and *ZMO0010* deletion mutants showed a slight decrease in biomass and growth rate with an increase of D-lactate titer. Knockout of the *ZMO1278* did not improve the performance of the strain, but instead affected its growth and D-lactate production (Table 1, Fig. 5B). Interestingly, the *ZMO1530* deletion mutant strain showed a significant decrease in biomass and growth rate but an increase in D-lactate production (Table 1, Fig. 5C). These results indicated that manipulation of *ZMO0902*, *ZMO1323*, *ZMO1044, ZMO0023*, *ZMO0010, ZMO0876,* and *ZMO1530* can improve the D-lactate production performance in *Z. mobilis*. Of all the mutants, D-lactate titers of *ZMO1323* and *ZMO1530* deletion mutant strains showed a significant 15% and 21% increase than that of the control strain (Table 1), respectively.

4. Discussion

Identification of gene targets and optimization of their expression are critical to achieving high titers and yields of the desired bioproducts through metabolic engineering [45]. However, gene-by-gene manipulation is time-consuming and inefficient due to our limitations on understanding of the metabolic and regulatory networks. Here, we established a biosensor-assisted CRISPRi high-throughput screening to identify potential genetic targets that play crucial roles in high D-lactate production quickly. The biosensor D-*lldR*-P_{lldp} could detect D-lactate in the range of 3~9 g/L with high correlations between fluorescence intensity and D-lactate concentrations ($R^2 > 0.98$). Coupled with genome-wide interference conducted by a CRISPRi library containing 69,093 crRNAs, we rapidly screened two strain libraries containing 10^5 and 10^4 mutants respectively from two rounds of FACS sorting, which is more efficient and comprehensive compared with gene-by-gene manipulation. These findings provide valuable insights into the underlying mechanisms and genetic components to facilitate the construction of recombinant strains with high titer of D-lactate production. The lldR-based biosensor used in this study can be directly employed for screening high D-lactate producer with a broad dynamic range for detecting low concentration of intracellular D-lactate. However, the ability of this biosensor can be further improved to detect D-lactic acid at high concentrations. Future research will focus on optimizing the biosensor using methods that have been developed recently including rational or semi-rational engineering based on protein structures [46], random mutant library generated by error-prone polymerase chain reaction (PCR) [47], laboratory directed evolution, *in vivo* continuous mutagenesis [48], transcriptional modifications [49–52], RBS sequences optimization at post-transcriptional level [53], and codon optimization [54].

Among the genes identified in this study, CRISPRi or deletion of *ZMO1323* and *ZMO1530* significantly improved D-lactate production. A BLASTP analysis of *ZMO1323* (Fig. S1A) and *ZMO1530* (Fig. S1B) using the NCBI database [55] showed that multiple species have homologous genes with high similarity with *ZMO1323* (Table S5) or *ZMO1530* (Table S6), respectively. *ZMO1323* encodes histidine protein kinase HPrK, which is involved in the regulation of sugar uptake and carbon metabolism [56]. HPrK catalyzes the phosphorylation of Ser46 of HPr to form P-Ser46-HPr, which acts as a co-repressor of the transcription of genes involved in carbohydrate transport and catabolism, including glycolysis [57,58]. A mutation of HPrK was found in a D-lactate tolerant *C. thermocellum* strain obtained through evolutionary engineering, indicating that HPrK might affect carbohydrate and/or phosphate metabolism [59]. We therefore proposed that the interference or deletion of HPrK in *Z. mobilis* released the repression of genes involved in carbohydrate transport and catabolism [56], thus enhancing the transport of D-lactate to the extracellular and D-lactate production. While *ZMO1530* encodes KpsF/GutQ family protein and participates in the carbohydrate metabolic process. Interference or deletion of *ZMO1*530 might help redirect metabolic carbon flux towards D-lactate production.

In this study, we established a biosensor-assisted CRISPRi high-throughput screening approach to identify genetic targets associated with high D-lactate production with two genes (*ZMO1323* and *ZMO1530*) contributing to high lactate production identified and confirmed, which can be applied to other microorganisms and extended for biochemicals with corresponding biosensors, such as butanol [60], citrate [61], L-glutamate [62], malate [63], methanol [64], resveratrol [65], pyruvate [66], and erythritol [67].

5. Conclusion

In this study, we developed a D-lactate biosensor-assisted CRISPRi high-throughput screening in *Z. mobilis* to identify potential genetic targets for high D-lactate production with two libraries containing 10^5

Table 1
Fermentation profiles of *ZMO0062*, *ZMO1044*, *ZMO1323, ZMO0023, ZMO0876, ZMO1278, ZMO0010, ZMO0902* and *ZMO1530* deficiency mutants. Mean values for triplicate repeats are shown for each condition ± standard deviation.

Strains	Growth rate	Glucose consumption ($g.L^{-1}$)	Ethanol titer ($g.L^{-1}$)	Lactate titer ($g.L^{-1}$)	Lactate productivity ($g.L^{-1}.h^{-1}$)	Carbon conversion rate (%)
HAPL	0.19 ± 0.01	80.99 ± 0.01	26.05 ± 0.03	27.71 ± 0.05	2.03 ± 0.02	98.6 ± 0.00
HAPLΔ0062	0.17 ± 0.01	79.33 ± 0.02	25.25 ± 0.24	27.92 ± 0.02	1.88 ± 0.03	98.9 ± 0.01
HAPLΔ1044	0.19 ± 0.02	82.17 ± 0.04	26.39 ± 0.21	28.34 ± 0.01	1.93 ± 0.02	98.7 ± 0.02
HAPLΔ1323	0.19 ± 0.02	81.92 ± 0.01	24.33 ± 0.02	31.85 ± 0.01	2.11 ± 0.01	98.3 ± 0.00
HAPLΔ0023	0.16 ± 0.01	82.13 ± 0.04	25.25 ± 0.34	29.92 ± 0.08	1.83 ± 0.03	97.9 ± 0.01
HAPLΔ0876	0.19 ± 0.02	78.93 ± 0.05	23.79 ± 0.25	30.36 ± 0.05	2.00 ± 0.02	98.8 ± 0.01
HAPLΔ1278	0.17 ± 0.01	83.27 ± 0.04	26.98 ± 1.02	27.05 ± 0.01	1.87 ± 0.01	97.3 ± 0.02
HAPLΔ0010	0.17 ± 0.02	81.99 ± 0.02	25.03 ± 0.04	30.11 ± 0.05	1.82 ± 0.02	97.8 ± 0.00
HAPLΔ0902	0.17 ± 0.01	82.14 ± 0.01	25.33 ± 0.04	29.89 ± 0.06	2.01 ± 0.03	98.1 ± 0.00
HAPLΔ1530	0.14 ± 0.01	80.96 ± 0.02	22.80 ± 0.02	33.52 ± 0.03	1.91 ± 0.02	97.7 ± 0.00

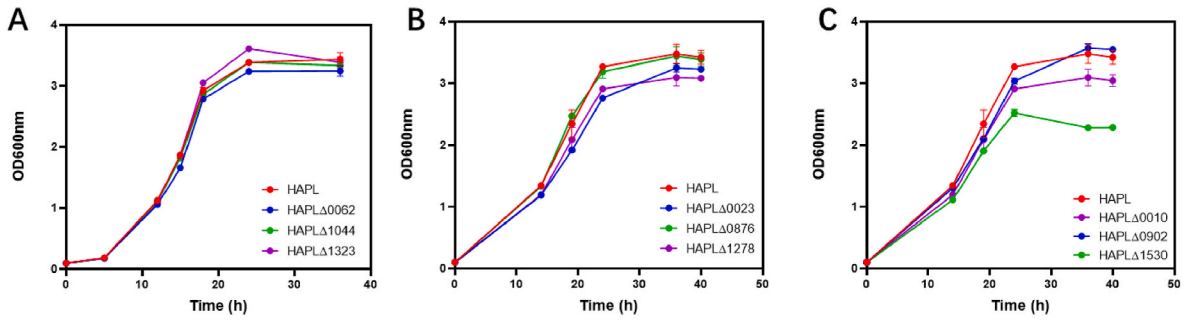

Fig. 5. Growth curve of *ZMO0062*, *ZMO1044*, *ZMO1323, ZMO0023, ZMO0876, ZMO1278, ZMO0010, ZMO0902,* and *ZMO1530* deficiency mutants. Values are the means of experiments with three technical replicates, error bars are standard deviation.

and 10^4 mutants obtained from two rounds of FACS screening respectively. Among them, 13 mutants with significant improvement in D-lactate production were then characterized, and two key genes were further confirmed to be associated with high D-lactate production by deletion or interference of their expression. This work thus established a D-lactate biosensor-assisted CRISPRi high-throughput screening to identify genetic targets associated with D-lactate production in *Z. mobilis*, which can not only be extended for other biochemicals with corresponding biosensors, but also provided a feasible high-throughput screening approach for rapid identification of genetic targets associated with strain performance in other microorganisms.

Funding

This work was supported by the National Key Research and Development Program of China (2022YFA0911800), National Natural Science Foundation of China (CN) (21978071), the Key Science and Technology Innovation Project of Hubei Province (2021BAD001), and the Innovation Base for Introducing Talents of Discipline of Hubei Province (2019BJH021). We also acknowledge the support from the State Key Laboratory of Biocatalysis and Enzyme Engineering.

CRediT authorship contribution statement

Qiqun Peng: Methodology, Investigation, Validation, Formal analysis, Data curation, Writing – original draft, Writing – review & editing. **Weiwei Bao:** Investigation, Validation, Formal analysis, Data curation, Writing – original draft. **Binan Geng:** Supervision, Resources, Writing – review & editing. **Shihui Yang:** Conceptualization, Project administration, Supervision, Funding acquisition, Writing – review & editing.

Declaration of competing interest

The authors declare that there are no known competing financial interests or personal relationships that could have appeared to influence the work reported in this paper.

Appendix A. Supplementary data

Supplementary data to this article can be found online at https://doi.org/10.1016/j.synbio.2024.02.002.

References

[1] Djukić-Vuković A, Mladenović D, Ivanović J, Pejin J, Mojović L. Towards sustainability of lactic acid and poly-lactic acid polymers production. Renew Sustain Energy Rev 2019;108:238–52. https://doi.org/10.1016/j.rser.2019.03.050.
[2] Grand view research. 2023. https://www.grandviewresearch.com/industryanalysis/lactic-acid-and-poly-lactic-acid-market [accessed 8 December 2023].
[3] Ma K, Cui Y, Zhao K, Yang Y, Wang Y, Hu G, et al. D-Lactic acid production from agricultural residues by membrane integrated continuous fermentation coupled with B vitamin supplementation. Biotechnol Biofuels Bioprod 2022;15(1):24. https://doi.org/10.1186/s13068-022-02124-y.
[4] Zhao X-Q, Liu C-G, Bai F-W. Making the biochemical conversion of lignocellulose more robust. Trends Biotechnol 2023. https://doi.org/10.1016/j.tibtech.2023.09.014.
[5] Wang Y, Cao W, Luo J, Wan Y. Exploring the potential of lactic acid production from lignocellulosic hydrolysates with various ratios of hexose versus pentose by *Bacillus coagulans* IPE22. Bioresour Technol 2018;261:342–9. https://doi.org/10.1016/j.biortech.2018.03.135.
[6] Okano K, Tanaka T, Ogino C, Fukuda H, Kondo A. Biotechnological production of enantiomeric pure lactic acid from renewable resources: recent achievements, perspectives, and limits. Appl Microbiol Biotechnol 2010;85(3):413–23. https://doi.org/10.1007/s00253-009-2280-5.
[7] Abdel-Rahman MA, Sonomoto K. Opportunities to overcome the current limitations and challenges for efficient microbial production of optically pure lactic acid. J Biotechnol 2016;236:176–92. https://doi.org/10.1016/j.jbiotec.2016.08.008.
[8] Shan W, Yan Y, Li Y, Hu W, Chen J. Microbial tolerance engineering for boosting lactic acid production from lignocellulose. Biotechnol Biofuels Bioprod 2023;16(1):78. https://doi.org/10.1186/s13068-023-02334-y.
[9] Wang X, He Q, Yang Y, Wang J, Haning K, Hu Y, et al. Advances and prospects in metabolic engineering of *Zymomonas mobilis*. Metab Eng 2018;50:57–73. https://doi.org/10.1016/j.ymben.2018.04.001.
[10] Yang S, Fei Q, Zhang Y, Contreras LM, Utturkar SM, Brown SD, et al. *Zymomonas mobilis* as a model system for production of biofuels and biochemicals. Microb Biotechnol 2016;9(6):699–717. https://doi.org/10.1111/1751-7915.12408.
[11] Yan X, Wang X, Yang Y, Wang Z, Zhang H, Li Y, et al. Cysteine supplementation enhanced inhibitor tolerance of *Zymomonas mobilis* for economic lignocellulosic bioethanol production. Bioresour Technol 2022;349:126878. https://doi.org/10.1016/j.biortech.2022.126878.
[12] Wu B, Qin H, Yang Y, Duan G, Yang S, Xin F, et al. Engineered *Zymomonas mobilis* tolerant to acetic acid and low pH via multiplex atmospheric and room temperature plasma mutagenesis. Biotechnol Biofuels 2019;12:10. https://doi.org/10.1186/s13068-018-1348-9.
[13] Li R, Shen W, Yang Y, Du J, Li M, Yang S. Investigation of the impact of a broad range of temperatures on the physiological and transcriptional profiles of *Zymomonas mobilis* ZM4 for high-temperature-tolerant recombinant strain development. Biotechnol Biofuels 2021;14(1):146. https://doi.org/10.1186/s13068-021-02000-1.
[14] Yang S, Mohagheghi A, Franden MA, Chou YC, Chen X, Dowe N, et al. Metabolic engineering of *Zymomonas mobilis* for 2,3-butanediol production from lignocellulosic biomass sugars. Biotechnol Biofuels 2016;9(1):189. https://doi.org/10.1186/s13068-016-0606-y.
[15] Hu M, Bao W, Peng Q, Hu W, Yang X, Xiang Y, et al. Metabolic engineering of *Zymomonas mobilis* for co-production of D-lactic acid and ethanol using waste feedstocks of molasses and corncob residue hydrolysate. Front Bioeng Biotechnol 2023;11:1135484. https://doi.org/10.3389/fbioe.2023.1135484.
[16] Shen W, Zhang J, Geng B, Qiu M, Hu M, Yang Q, et al. Establishment and application of a CRISPR-Cas12a assisted genome-editing system in *Zymomonas mobilis*. Microb Cell Factories 2019;18(1):162. https://doi.org/10.1186/s12934-019-1219-5.
[17] Zheng Y, Han J, Wang B, Hu X, Li R, Shen W, et al. Characterization and repurposing of the endogenous Type I-F CRISPR-Cas system of *Zymomonas mobilis* for genome engineering. Nucleic Acids Res 2019;47(21):11461–75. https://doi.org/10.1093/nar/gkz940.
[18] Wu J, Du G, Chen J, Zhou J. Enhancing flavonoid production by systematically tuning the central metabolic pathways based on a CRISPR interference system in *Escherichia coli*. Sci Rep 2015;5:13477. https://doi.org/10.1038/srep13477.
[19] Wu MY, Sung LY, Li H, Huang CH, Hu YC. Combining CRISPR and CRISPRi systems for metabolic engineering of *E. coli* and 1,4-BDO biosynthesis. ACS Synth Biol 2017;6(12):2350–61. https://doi.org/10.1021/acssynbio.7b00251.
[20] Lu Z, Yang S, Yuan X, Shi Y, Ouyang L, Jiang S, et al. CRISPR-assisted multi-dimensional regulation for fine-tuning gene expression in *Bacillus subtilis*. Nucleic Acids Res 2019;47(7):e40. https://doi.org/10.1093/nar/gkz072.
[21] Ni J, Zhang G, Qin L, Li J, Li C. Simultaneously down-regulation of multiplex branch pathways using CRISPRi and fermentation optimization for enhancing

β-amyrin production in *Saccharomyces cerevisiae*. Synth Syst Biotechnol 2019;4(2):79–85. https://doi.org/10.1016/j.synbio.2019.02.002.
[22] Cleto S, Jensen JV, Wendisch VF, Lu TK. *Corynebacterium glutamicum* metabolic engineering with CRISPR interference (CRISPRi). ACS Synth Biol 2016;5(5):375–85. https://doi.org/10.1021/acssynbio.5b00216.
[23] Liu L, Helal SE, Peng N. CRISPR-Cas-based engineering of probiotics. Biodes Res 2023;5:0017. https://doi.org/10.34133/bdr.0017.
[24] Tian X, Chen H, Liu H, Chen J. Recent advances in lactica cid production by lactic acid bacteria. Appl Biochem Biotechnol 2021;193(12):4151–71. https://doi.org/10.1007/s12010-021-03672-z.
[25] Lv X, Xue H, Qin L, Li C. Transporter engineering in microbial cell factory boosts biomanufacturing capacity. Biodes Res 2022;2022:9871087. https://doi.org/10.34133/2022/9871087.
[26] Koivuranta KT, Ilmén M, Wiebe MG, Ruohonen L, Suominen P, Penttilä M. L-lactic acid production from D-xylose with *Candida sonorensis* expressing a heterologous lactate dehydrogenase encoding gene. Microb Cell Factories 2014;13:107. https://doi.org/10.1186/s12934-014-0107-2.
[27] Ilmén M, Koivuranta K, Ruohonen L, Rajgarhia V, Suominen P, Penttilä M. Production of L-lactic acid by the yeast *Candida sonorensis* expressing heterologous bacterial and fungal lactate dehydrogenases. Microb Cell Factories 2013;12:53. https://doi.org/10.1186/1475-2859-12-53.
[28] Suzuki T, Sakamoto T, Sugiyama M, Ishida N, Kambe H, Obata S, et al. Disruption of multiple genes whose deletion causes lactic-acid resistance improves lactic-acid resistance and productivity in *Saccharomyces cerevisiae*. J Biosci Bioeng 2013;115(5):467–74. https://doi.org/10.1016/j.jbiosc.2012.11.014.
[29] Abdullah Al M, Sugimoto S, Higashi C, Matsumoto S, Sonomoto K. Improvement of multiple-stress tolerance and lactic acid production in *Lactococcus lactis* NZ9000 under conditions of thermal stress by heterologous expression of *Escherichia coli* DnaK. Appl Environ Microbiol 2010;76(13):4277–85. https://doi.org/10.1128/aem.02878-09.
[30] Park JM, Kim TY, Lee SY. Constraints-based genome-scale metabolic simulation for systems metabolic engineering. Biotechnol Adv 2009;27(6):979–88. https://doi.org/10.1016/j.biotechadv.2009.05.019.
[31] Wang J, Li C, Jiang T, Yan Y. Biosensor-assisted titratable CRISPRi high-throughput (BATCH) screening for over-production phenotypes. Metab Eng 2023;75:58–67. https://doi.org/10.1016/j.ymben.2022.11.004.
[32] Liu D, Evans T, Zhang F. Applications and advances of metabolite biosensors for metabolic engineering. Metab Eng 2015;31:35–43. https://doi.org/10.1016/j.ymben.2015.06.008.
[33] Crnković T, Bokor BJ, Lockwood ME, Cornish VW. Peptide variant detection by a living yeast biosensor via an epitope-selective protease. Biodes Res 2023;5:3. https://doi.org/10.34133/bdr.0003.
[34] Liu Y, Yuan G, Hassan MM, Abraham PE, Mitchell JC, Jacobson D, et al. Biological and molecular components for genetically engineering biosensors in plants. Biodes Res 2022;2022:9863496. https://doi.org/10.34133/2022/9863496.
[35] Augustiniene E, Malys N. Identification and characterization of L- and D-lactate-inducible systems from *Escherichia coli* MG1655, *Cupriavidus necator* H16 and *Pseudomonas* species. Sci Rep 2022;12(1):2123. https://doi.org/10.1038/s41598-022-06028-7.
[36] Nasu Y, Murphy-Royal C, Wen Y, Haidey JN, Molina RS, Aggarwal A, et al. A genetically encoded fluorescent biosensor for extracellular L-lactate. Nat Commun 2021;12(1):7058. https://doi.org/10.1038/s41467-021-27332-2.
[37] Singh K, Ainala SK, Kim Y, Park S. A novel D(-)-lactic acid-inducible promoter regulated by the GntR-family protein D-LldR of *Pseudomonas fluorescens*. Synth Syst Biotechnol 2019;4(3):157–64. https://doi.org/10.1016/j.synbio.2019.08.004.
[38] Xia Y, Li K, Li J, Wang T, Gu L, Xun L. T5 exonuclease-dependent assembly offers a low-cost method for efficient cloning and site-directed mutagenesis. Nucleic Acids Res 2019;47(3):e15. https://doi.org/10.1093/nar/gky1169.
[39] Bao W, Shen W, Peng Q, Du J, Yang S. Metabolic engineering of *Zymomonas mobilis* for acetoin production by carbon redistribution and cofactor balance. Fermentation 2023;9(2):113.
[40] Yang Y, Shen W, Huang J, Li R, Xiao Y, Wei H, et al. Prediction and characterization of promoters and ribosomal binding sites of *Zymomonas mobilis* in system biology era. Biotechnol Biofuels 2019;12:52. https://doi.org/10.1186/s13068-019-1399-6.
[41] Yang TT, Cheng L, Kain SR. Optimized codon usage and chromophore mutations provide enhanced sensitivity with the green fluorescent protein. Nucleic Acids Res 1996;24(22):4592–3. https://doi.org/10.1093/nar/24.22.4592.
[42] Song H, Yang Y, Li H, Du J, Hu Z, Chen Y, et al. Determination of nucleotide sequences within promoter regions affecting promoter compatibility between *Zymomonas mobilis* and *Escherichia coli*. ACS Synth Biol 2022;11(8):2811–9. https://doi.org/10.1021/acssynbio.2c00187.
[43] Yang S, Vera JM, Grass J, Savvakis G, Moskvin OV, Yang Y, et al. Complete genome sequence and the expression pattern of plasmids of the model ethanologen *Zymomonas mobilis* ZM4 and its xylose-utilizing derivatives 8b and 2032. Biotechnol Biofuels 2018;11:125. https://doi.org/10.1186/s13068-018-1116-x.
[44] Yang S, Tschaplinski TJ, Engle NL, Carroll SL, Martin SL, Davison BH, et al. Transcriptomic and metabolomic profiling of *Zymomonas mobilis* during aerobic and anaerobic fermentations. BMC Genom 2009;10:34. https://doi.org/10.1186/1471-2164-10-34.
[45] Ko YS, Kim JW, Lee JA, Han T, Kim GB, Park JE, et al. Tools and strategies of systems metabolic engineering for the development of microbial cell factories for chemical production. Chem Soc Rev 2020;49(14):4615–36. https://doi.org/10.1039/d0cs00155d.
[46] Li Y, Reed M, Wright HT, Cropp TA, Williams GJ. Development of genetically encoded biosensors for reporting the methyltransferase-dependent biosynthesis of semisynthetic macrolide antibiotics. ACS Synth Biol 2021;10(10):2520–31. https://doi.org/10.1021/acssynbio.1c00151.
[47] Snoek T, Chaberski EK, Ambri F, Kol S, Bjørn SP, Pang B, et al. Evolution-guided engineering of small-molecule biosensors. Nucleic Acids Res 2020;48(1):e3. https://doi.org/10.1093/nar/gkz954.
[48] Javanpour AA, Liu CC. Evolving small-molecule biosensors with improved performance and reprogrammed ligand preference using orthoRep. ACS Synth Biol 2021;10(10):2705–14. https://doi.org/10.1021/acssynbio.1c00316.
[49] De Mey M, Maertens J, Lequeux GJ, Soetaert WK, Vandamme EJ. Construction and model-based analysis of a promoter library for *E. coli*: an indispensable tool for metabolic engineering. BMC Biotechnol 2007;7:34. https://doi.org/10.1186/1472-6750-7-34.
[50] Block DH, Hussein R, Liang LW, Lim HN. Regulatory consequences of gene translocation in bacteria. Nucleic Acids Res 2012;40(18):8979–92. https://doi.org/10.1093/nar/gks694.
[51] Murphy KF, Balázsi G, Collins JJ. Combinatorial promoter design for engineering noisy gene expression. Proc Natl Acad Sci USA 2007;104(31):12726–31. https://doi.org/10.1073/pnas.0608451104.
[52] Shis DL, Bennett MR. Library of synthetic transcriptional AND gates built with split T7 RNA polymerase mutants. Proc Natl Acad Sci USA 2013;110(13):5028–33. https://doi.org/10.1073/pnas.1220157110.
[53] Salis HM, Mirsky EA, Voigt CA. Automated design of synthetic ribosome binding sites to control protein expression. Nat Biotechnol 2009;27(10):946–50. https://doi.org/10.1038/nbt.1568.
[54] Welch M, Govindarajan S, Ness JE, Villalobos A, Gurney A, Minshull J, et al. Design parameters to control synthetic gene expression in *Escherichia coli*. PLoS One 2009;4(9):e7002. https://doi.org/10.1371/journal.pone.0007002.
[55] Altschul SF, Madden TL, Schäffer AA, Zhang J, Zhang Z, Miller W, et al. Gapped BLAST and PSI-BLAST: a new generation of protein database search programs. Nucleic Acids Res 1997;25(17):3389–402. https://doi.org/10.1093/nar/25.17.3389.
[56] Deutscher J, Aké FM, Derkaoui M, Zébré AC, Cao TN, Bouraoui H, et al. The bacterial phosphoenolpyruvate:carbohydrate phosphotransferase system: regulation by protein phosphorylation and phosphorylation-dependent protein-protein interactions. Microbiol Mol Biol Rev 2014;78(2):231–56. https://doi.org/10.1128/mmbr.00001-14.
[57] Shimizu K, Matsuoka Y. Regulation of glycolytic flux and overflow metabolism depending on the source of energy generation for energy demand. Biotechnol Adv 2019;37(2):284–305. https://doi.org/10.1016/j.biotechadv.2018.12.007.
[58] Fieulaine S, Morera S, Poncet S, Monedero V, Gueguen-Chaignon V, Galinier A, et al. X-ray structure of HPr kinase: a bacterial protein kinase with a P-loop nucleotide-binding domain. EMBO J 2001;20(15):3917–27. https://doi.org/10.1093/emboj/20.15.3917.
[59] Mazzoli R, Olson DG, Concu AM, Holwerda EK, Lynd LR. *In vivo* evolution of lactic acid hyper-tolerant *Clostridium thermocellum*. Nat Biotechnol 2022;67:12–22. https://doi.org/10.1016/j.nbt.2021.12.003.
[60] Yang Y, Lang N, Zhang L, Wu H, Jiang W, Gu Y. A novel regulatory pathway consisting of a two-component system and an ABC-type transporter contributes to butanol tolerance in *Clostridium acetobutylicum*. Appl Microbiol Biotechnol 2020;104(11):5011–23. https://doi.org/10.1007/s00253-020-10555-6.
[61] Yamamoto K, Matsumoto F, Oshima T, Fujita N, Ogasawara N, Ishihama A. Anaerobic regulation of citrate fermentation by CitAB in *Escherichia coli*. Biosci Biotechnol Biochem 2008;72(11):3011–4. https://doi.org/10.1271/bbb.80301.
[62] Lundgren BR, Shoytush JM, Scheel RA, Sain S, Sarwar Z, Nomura CT. Utilization of L-glutamate as a preferred or sole nutrient in *Pseudomonas aeruginosa* PAO1 depends on genes encoding for the enhancer-binding protein AauR, the sigma factor RpoN and the transporter complex AatJQMP. BMC Microbiol 2021;21(1):83. https://doi.org/10.1186/s12866-021-02145-x.
[63] Tanaka K, Kobayashi K, Ogasawara N. The *Bacillus subtilis* YufLM two-component system regulates the expression of the malate transporters MaeN (YufR) and YflS, and is essential for utilization of malate in minimal medium. Microbiology 2003;149(Pt 9):2317–29. https://doi.org/10.1099/mic.0.26257-0.
[64] Ganesh I, Vidhya S, Eom GT, Hong SH. Construction of methanol-sensing *Escherichia coli* by the introduction of a *Paracoccus denitrificans* MxaY-based chimeric two-component system. J Microbiol Biotechnol 2017;27(6):1106–11. https://doi.org/10.4014/jmb.1611.11070.
[65] Sun H, Zhao H, Ang EL. A new biosensor for stilbenes and a cannabinoid enabled by genome mining of a transcriptional regulator. ACS Synth Biol 2020;9(4):698–705. https://doi.org/10.1021/acssynbio.9b00443.
[66] Xu X, Li X, Liu Y, Zhu Y, Li J, Du G, et al. Pyruvate-responsive genetic circuits for dynamic control of central metabolism. Nat Chem Biol 2020;16(11):1261–8. https://doi.org/10.1038/s41589-020-0637-3.
[67] Qiu X, Xu P, Zhao X, Du G, Zhang J, Li J. Combining genetically-encoded biosensors with high throughput strain screening to maximize erythritol production in *Yarrowia lipolytica*. Metab Eng 2020;60:66–76. https://doi.org/10.1016/j.ymben.2020.03.006.